Supporting Information:

Alkaline hydrogel electrolyte from biosourced chitosan to enhance the rate capability and energy density of carbon-based supercapacitors

Sirine Zallouz[1,2], Jean-Marc Le Meins[1,2], Camélia Matei Ghimbeu[1,2,3,]*

[1] Université de Haute-Alsace, CNRS, Institut de Science des Matériaux de Mulhouse (IS2M) UMR 7361, F-68100 Mulhouse, France

[2] Université de Strasbourg, F-67081 Strasbourg, France

[3] Réseau sur le stockage Electrochimique de l'Energie (RS2E), FR CNRS 3459, 80039 Amiens Cedex, France

*Corresponding author:

E-mail address: camelia.ghimbeu@uha.fr (C. Matei Ghimbeu).

Tel: + 33 (0) 3 89 60 87 43

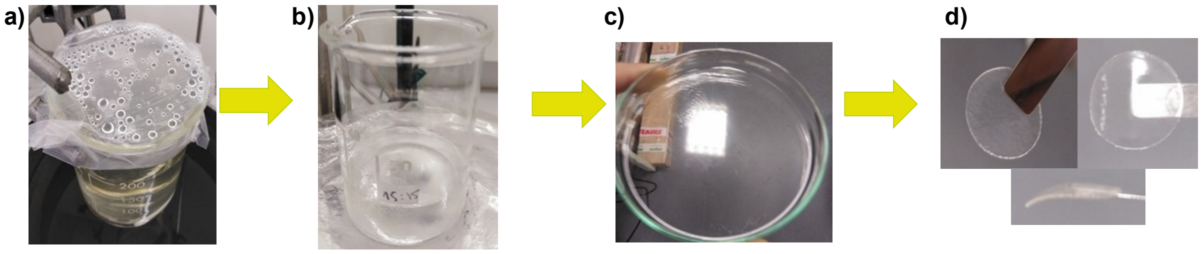

Figure S1: Pictures of chitosan-KOH gel electrolyte preparation, showing the main involved steps: a) chitosan polymer host + solvent solution: reticulation b) solution after 2 M KOH electrolyte addition; c) solution casting in Petri dish; d) hydrogel cutting.

For the textural properties analysis, the samples (~100 mg) were outgassed under vacuum at 300 °C for 12 h on the degassing port and subsequently for another 2 h on the analysis port at the same temperature, then we subjected them to N_2 adsorption. The specific surface area (S_{BET}) was calculated from the linear plot at the relative pressure range of 0.05-0.3 using the BET (Brunauer-Emmett-Teller) model. The micropore volume (V_{micro}) was determined by the Dubinin-Radushkevich (DR) equation, while the mesopore volume (V_{meso}) was obtained by substracting the micropore volume from the total pore volume (V_T) of N_2 adsorbed at relative pressure P/P_0 equal to 0.95. Pore size distribution was evaluated using the adsorption isotherm branch and the 2D-NLDFT (non-local density functional theory) heterogeneous surface pore model for carbon materials explored in SAIEUS software.[1]

Table S1: Textural properties of activated carbon Norit R3 extra using N_2 adsorption at 77 K.

Material	S_{BET} (m^2 g^{-1})	V_T (cm^3 g^{-1})	V_{micro} (cm^3 g^{-1})	V_{meso} (cm^3 g^{-1})
Norit R3 Extra	1224	0.56	0.47	0.09

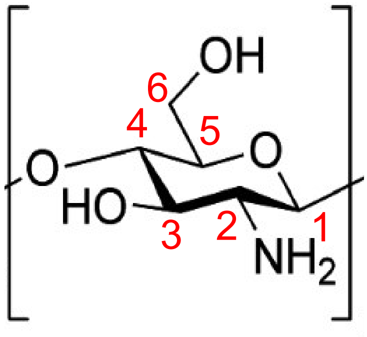

Figure S2: Chemical structure of chitosan.

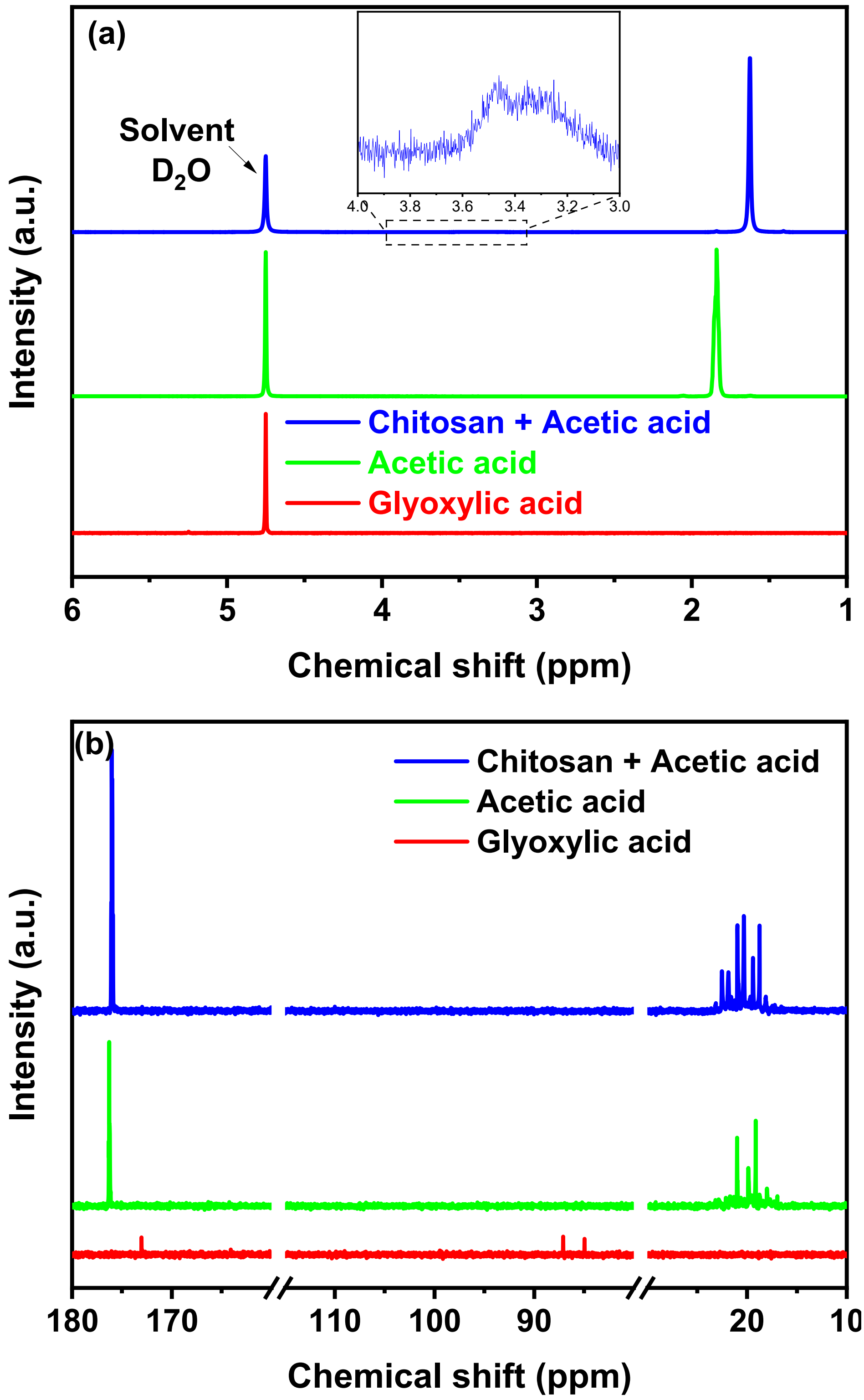

Figure S3: (a) ^{1}H NMR (inset: ^{1}H NMR from 3 – 4 ppm), (b) ^{13}C NMR of precursors used in the preparation of chitosan-KOH gel electrolyte.

The conductivity (σ) was calculated using the following formula:

$$\sigma = \frac{L}{R * A}$$

Where L is the thickness of the self-standing gel-electrolyte (cm), R is the resistance given by EIS (Ω) and A is the surface of the self-standing gel-electrolyte in contact with electrode (cm^2). The result is given in S cm^{-1}. The resistance R has been measured by EIS in several places and the average value has been used.

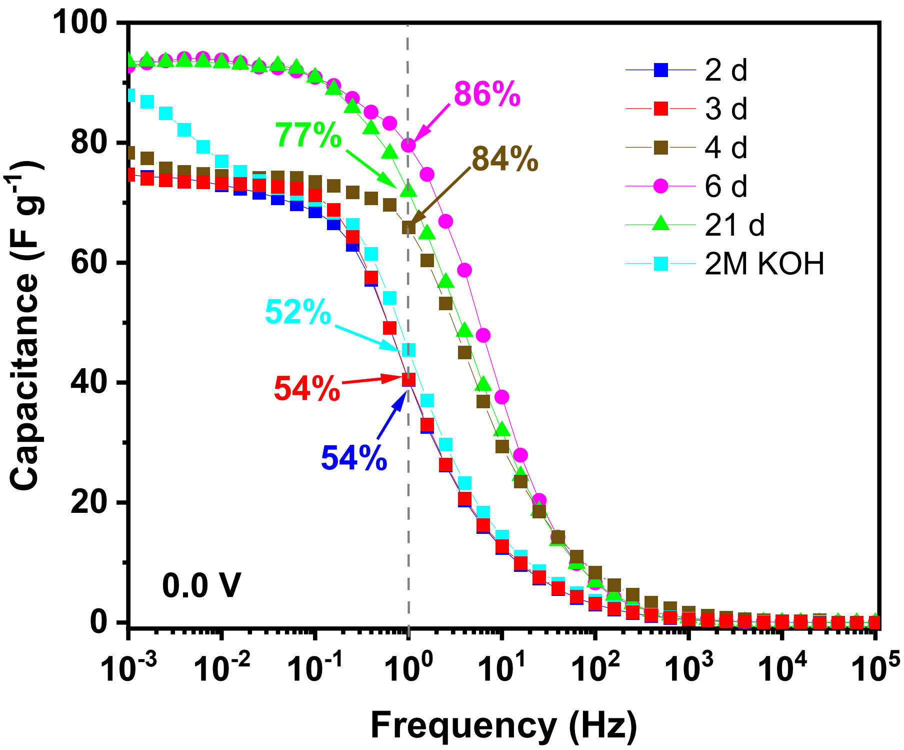

Figure S4: Capacitance vs. frequency for activated carbon using different chitosan-KOH electrolyte solution aged for different time periods and liquid KOH 2 M.

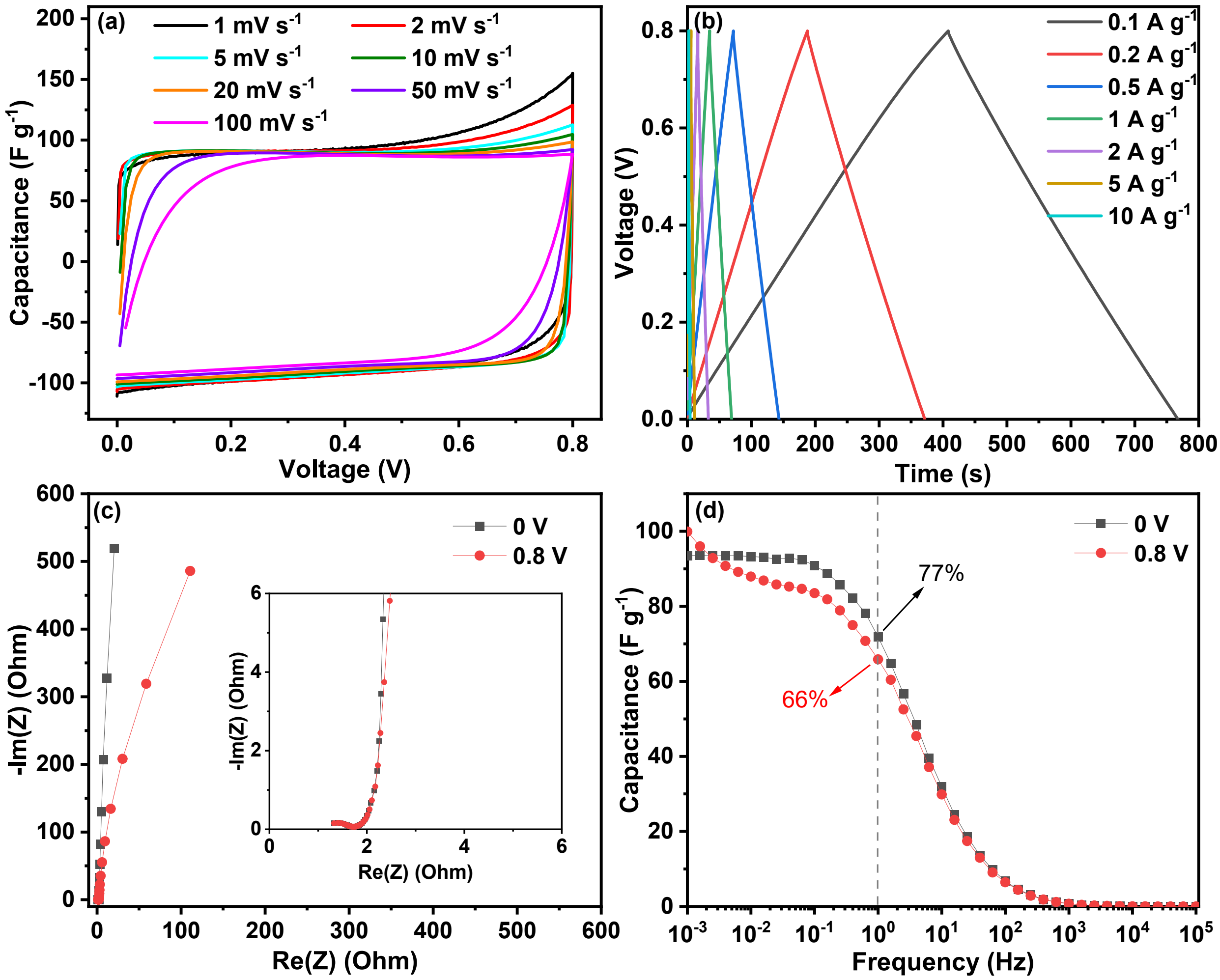

Figure S5: Electrochemical performance with of carbon-carbon supercapacitor using chitosan-KOH gel electrolyte (21 d) at a voltage of 0.8 V; (a) cyclic voltammetry at different sweep rates; (b) galvanostatic charge discharge at different current densities; (c) Nyquist plot from electrochemical impedance spectroscopy; (d) capacitance vs frequency from electrochemical impedance spectroscopy.

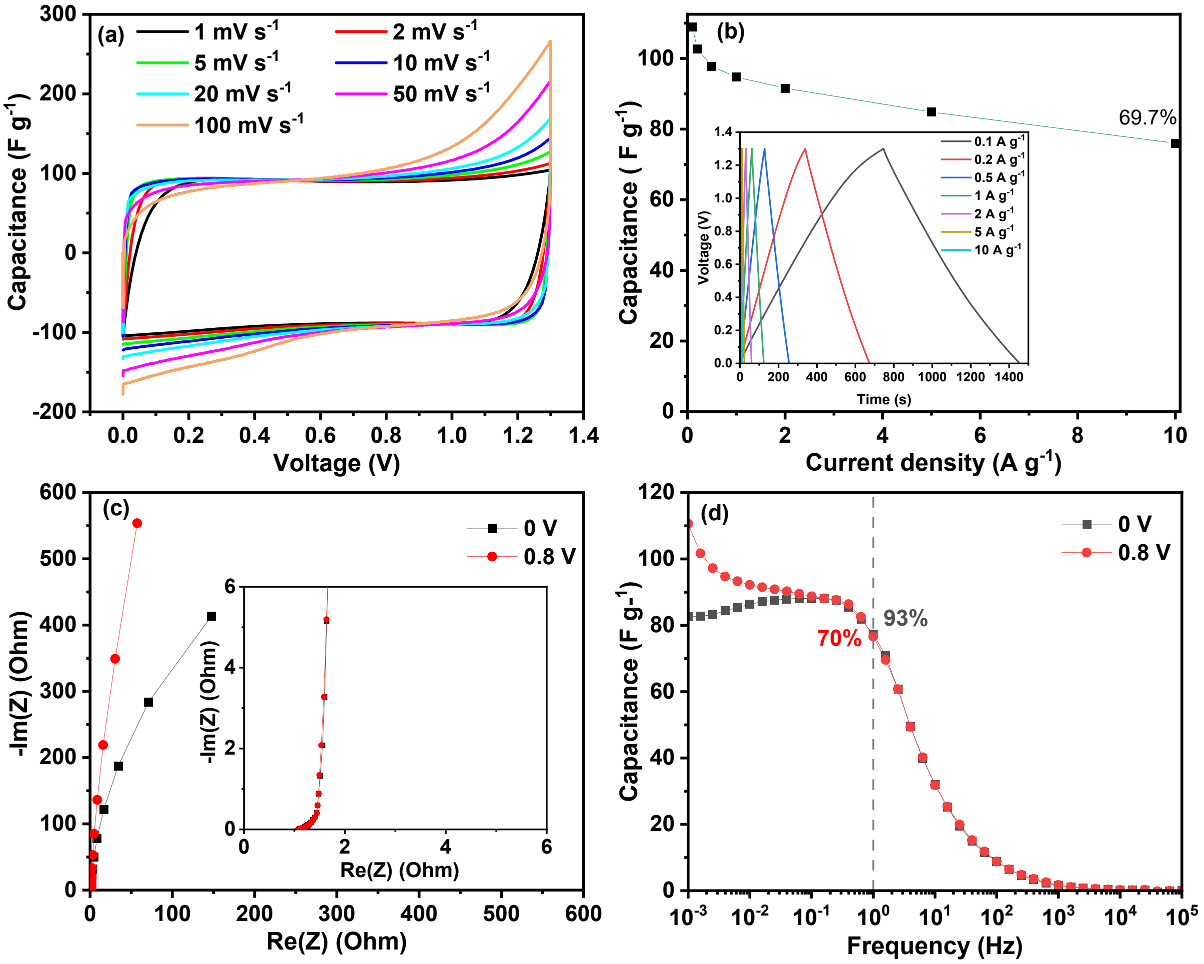

Figure S6: Electrochemical performance with of carbon-carbon supercapacitor using chitosan-KOH gel electrolyte (4 d) at a voltage of 1.3 V: (a) cyclic voltammetry at different sweep rates; (b) Rate capability at different current densities (inset: galvanostatic charge discharge at different current densities); (c) Nyquist plot from electrochemical impedance spectroscopy; (d) Capacitance vs frequency from electrochemical impedance spectroscopy.

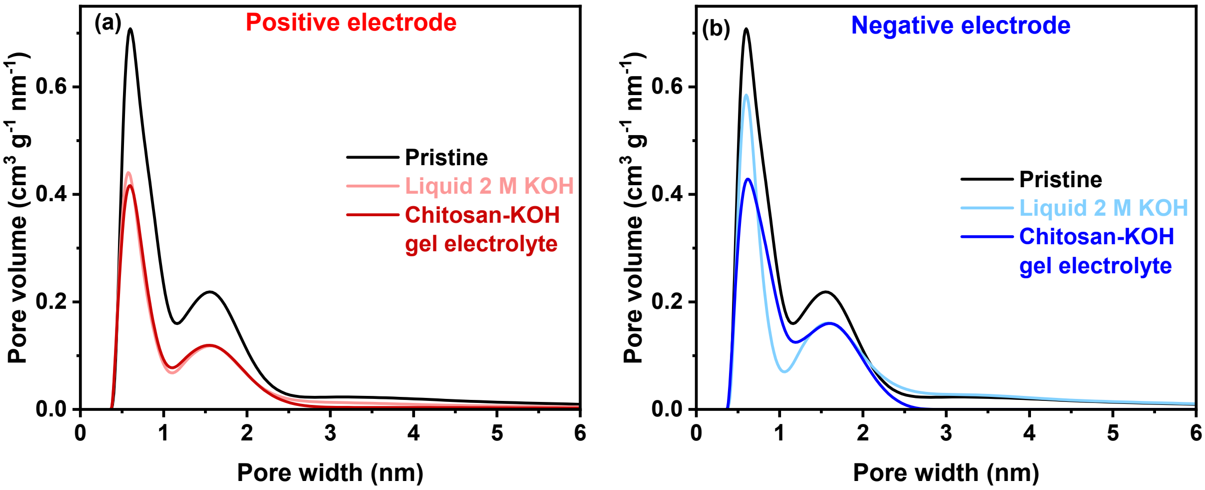

Figure S7: Pore size distribution using the 2D-NLDFT heterogeneous surface carbon model in the SAIEUS software for (a) pristine and positive electrodes; (b) pristine and negative electrodes after voltage window widening to 1.4 V.

Table S2: Electrochemical performance of different electrochemical capacitors using different gel electrolytes based on aqueous electrolytes.

Polymer/ Gelling agent	Electrolyte	Gel thickness	Type of electrochemical cell	Electrode active material	Voltage window (V)	Capacitance at current load	Energy and power	References
Polyvinyl alcohol (PVA)	Na_2SO_4 1 M	300 µm	Symmetric two and three electrode	Microporous activated carbon	1.8	135 F g^{-1} at 1 A g^{-1}	13 W h kg^{-1} at 100 W kg^{-1}	[2]
Agar	K_2SO_4 0.5 M	200 µm	Symmetric two and three electrode	Activated carbon Kynol 507-20	1.6	100 F g^{-1} at 1 A g^{-1}	8 W h kg^{-1} at 100 W kg^{-1}	[3]
Polyvinyl alcohol (PVA)	H_3PO_4 1.5 M	-	Symmetric solid state supercapacitor	Single walled carbon nanotubes	0.8	45 F g^{-1} at 0.1 A g^{-1}	0,9 W h kg^{-1} at 10,5 W kg^{-1}	[4]
PVA	KOH 0.5 M	-	Symmetric quasi solid state supercapacitor	Hierarchical porous self-doped carbon	1	177 F g^{-1} at 0.1 A g^{-1}	7.3 W h kg^{-1} at 125.1	[5]

							W kg^{-1}	
Chitosan	Li_2SO_4 1 M	~100 µm	Symmetric quasi solid state supercapacitor	Activated carbon	1.4	31.89 F g^{-1} at 0.5 A g^{-1}	8.7 Wh kg^{-1} at 350.3 W kg^{-1}	[6]
Chitosan	KOH 1 M	~ 100 µm	Symmetric quasi solid state supercapacitor	Carbon cloth	0.9	39.11 F g^{-1} at 0.5 A g^{-1}	4.39 Wh kg^{-1} at 224.99 W kg^{-1}	[7]
Chitosan	KOH 2 M	200 µm	Symmetric two electrodes	Activated carbon Norit R3 extra	1.3	109 F g^{-1} at 0.1 A g^{-1}	5.1 W h kg^{-1} at 32.5 W kg^{-1}	This work

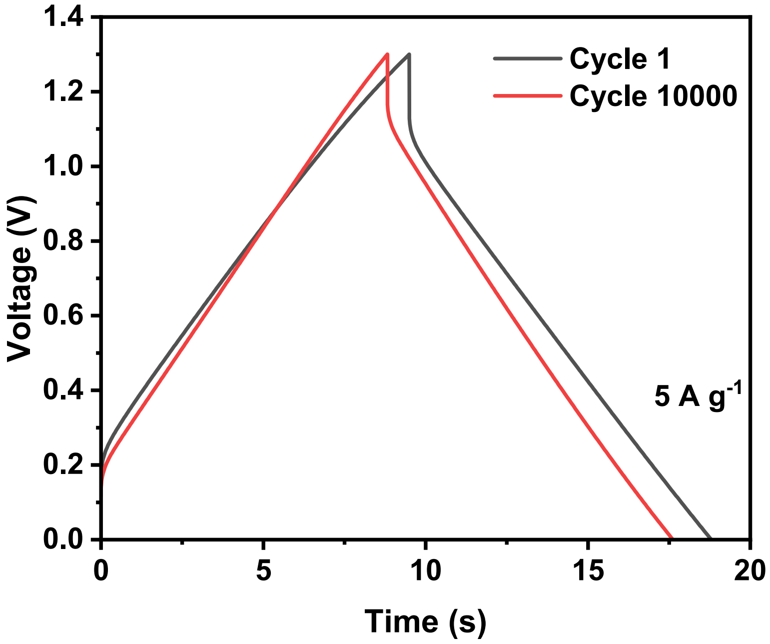

Figure S8: Comparison of charge discharge profiles of chitosan-KOH gel electrolyte (20 d) at a voltage of 1.3 V for long cycling at 5 A g^{-1}.

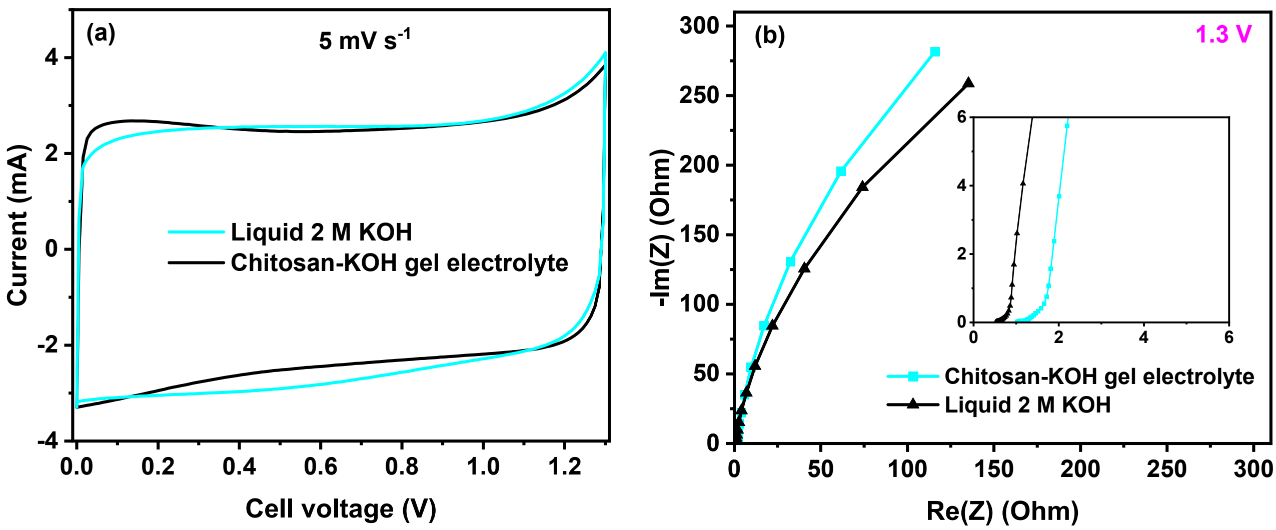

Figure S9: Electrochemical measurements after cycling for 10000 cycles at 1.3 V with a current load of 5 A g^{-1} for electrochemical capacitor using liquid 2 M KOH and chitosan-KOH gel electrolyte: (a) Cyclic voltammetry at 5 mv s^{-1} (b) Potentiostatic electrochemical impedance spectroscopy at 1.3 V.

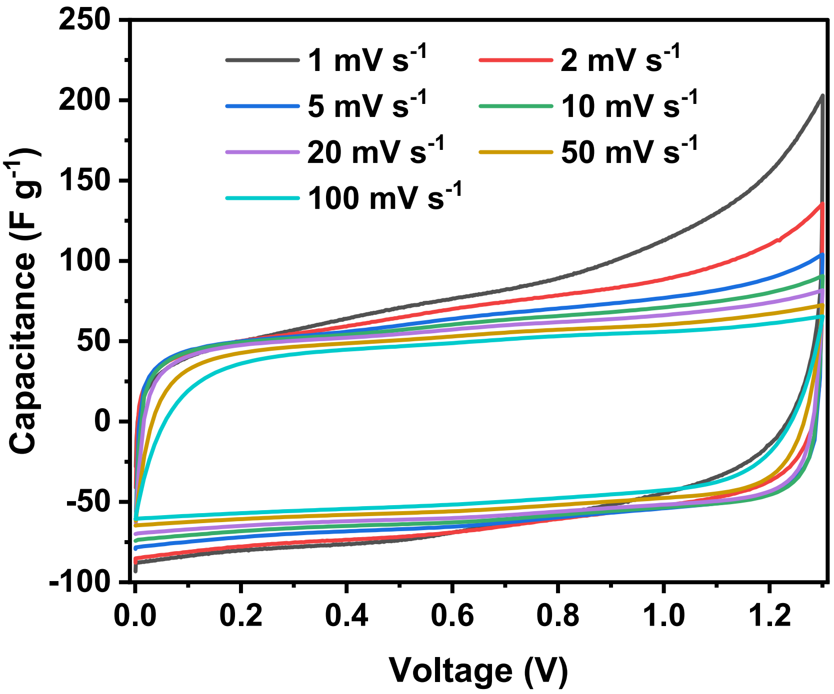

Figure S10: Cyclic voltammetry of chitosan-KOH gel electrolyte with C/Co_3O_4 750-230 nanocomposite at different sweep rates.

References:

1 S. Zallouz, B. Réty, L. Vidal, J.-M. Le Meins and C. Matei Ghimbeu, *ACS Appl. Nano Mater.*, DOI:10.1021/acsanm.1c00522.
2 N. Batisse and E. Raymundo-Piñero, *Journal of Power Sources*, 2017, **348**, 168–174.
3 J. Menzel, E. Frąckowiak and K. Fic, *Electrochimica Acta*, 2020, **332**, 135435.
4 S. Hong, H. Kim, S. Gao, R. L. Lavall, H. Y. Jung and Y. J. Jung, *Journal of Power Sources*, 2019, **432**, 16–23.
5 Z. Li, S. Gao, H. Mi, C. Lei, C. Ji, Z. Xie, C. Yu and J. Qiu, *Carbon*, 2019, **149**, 273–280.
6 H. Yang, X. Ji, Y. Tan, Y. Liu and F. Ran, *Journal of Power Sources*, 2019, **441**, 227174.
7 Q. Zhang, L. Zhao, H. Yang, L. Kong and F. Ran, *Journal of Membrane Science*, 2021, **629**, 119083.